

4. S. Z. Dunin and V. K. Sirotkin, "Expansion of a gas cavity in brittle rock taking account of the dilatancy properties of the soil," *Zh. Prikl. Mekh. Tekh. Fiz.*, No. 4 (1977).
5. V. I. Rodionov et al., *Mechanical Effect of an Underground Explosion* [in Russian], Moscow (1971).
6. P. Chadwick, A. Cox, and G. Hopkins, *Mechanics of Deep Underground Explosions* [Russian translation], Mir, Moscow (1966).
7. V. N. Nikolaevskii and N. M. Syrnikov, "On a plane limit flow of a friable dilating medium," *Izv. Akad. Nauk SSSR, Mekh. Tverd. Tela*, No. 2 (1970).

MODEL OF THE SOIL AND COMPUTATIONAL COMPLEX  
FOR THE ANALYSIS OF UNDERGROUND EXPLOSIONS

V. V. Bashurov, Yu. S. Vakhrameev,  
S. V. Dem'yanovskii, V. V. Ignatenko,  
and T. V. Simonova

UDC 518.12:539.3

In underground explosions executed in the interests of ejection, downcomer funnel or bulging hillock formation, the soil properties influence not only the quantitative parameters substantially, but also the qualitative pattern of the explosion. Thus, under the same conditions of charge embedding and power, a downcomer funnel or bulging hillock can be formed depending on the properties of the rock. The majority of explosions are performed in hard rock. Hence, the model of the soil should be suitable to describe its fundamental properties. A model of rocky soil is presented in this paper, the scheme for a numerical computation of the problem is described, and results of certain computations are presented.

1. An unruptured medium is considered elastic. Rupture sets in instantaneously upon the attainment of definite criteria. Right after rupture, which occurs in brittle material under insignificant strains, the pulverized rock consists of separate compactly contiguous pieces. In this state its volume density is 1.5-1.7 times greater than in rubble fill. The compact fractured medium and loose rubble differ quite radically in the effective value of the internal friction and ~100 times in the volume compressibility. It is hence important to take account of the gradual change in the properties of the ruptured medium as it loosens.

In both states, before and after rupture, the medium is considered isotropic. The pressure and degree of looseness are taken as parameters of the state in this model. The influence on the mechanical properties of the size of the pieces, their shape, and temperature are neglected.

The equations of state of a ruptured medium are written in differential form. The change in density is defined by the equation

$$d\rho/\rho = d\rho/K_{1,2}(\rho, \rho) - \Phi(\rho, \rho)\sqrt{J_2}dt. \quad (1.1)$$

where  $J_2$  is the second invariant of the strain rate deviator.

The first term on the right corresponds to pure volume strain, while the second describes the dilatancy effect. An analogous equation was examined in [1] in application to friable media and soft soils. In this paper (1.1) is extended to all states of ruptured rocky soil, including rubble, and a state with dense packing. Hence,  $K_{1,2}$  and  $\Phi$  are understood to be strongly varying functions of their arguments. The irreversibility of the volume strain is taken into account by the fact that the absolute value of the volume compressibility  $K_{1,2}$  depends on the sign of  $d\rho$ . In the construction of the function  $\Phi(\rho, \rho)$  it is assumed for simplicity that:

- a) for  $d\rho=0$  the shear strains result only in loosening of the substance;
- b) the loosening intensity vanishes at the extreme curve  $p_2(\rho)$  (Fig. 1) corresponding to monotonic compression of the loosest rubble. The domain of possible states of the ruptured medium is shown in Fig. 1.

---

Chelyabinsk. Translated from *Zhurnal Prikladnoi Mekhaniki i Tekhnicheskoi Fiziki*, No. 3, pp. 153-160, May-June, 1979. Original article submitted December 27, 1977.

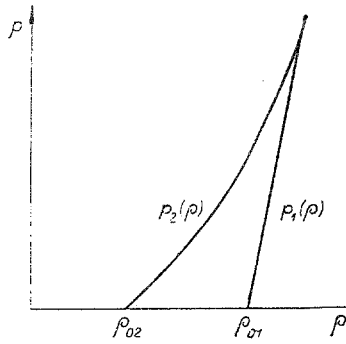


Fig. 1

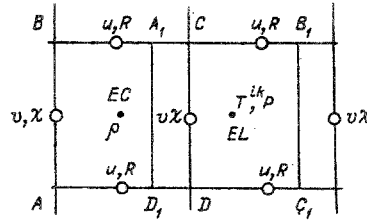


Fig. 2

For an unruptured medium  $K_1 = K_2$  and  $\Phi(p, \rho) = 0$ ; i.e., there is no loosening, and the pressure is a single-valued function of the density  $p = p_1(\rho)$ . At high pressures the curves  $p_2(\rho)$  and  $p_1(\rho)$  join. Under these assumptions, points on the  $(\rho, p)$  plane corresponding to the state of the ruptured medium, are included between  $p_2(\rho)$ ,  $p_1(\rho)$ , and  $p = 0$  within the curvilinear triangle, where the passage between any two points is possible because of the different combination of volume and shear strains.

If  $p = 0$  in the travel state, the mean volume density can be less than  $\rho_{02}$ . The instantaneous magnitude of the volume density does not yield a conception of the nature of the piece arrangement. The value of the density  $\rho^*$  is taken as the state parameter, and when it is reached in this substances if uniformly compressed, a positive pressure occurs. The computation of  $\rho^*$  is performed by means of an equation analogous to (1.1):

$$d\rho^*/\rho^* = -\Phi(0, \rho^*)\sqrt{J_2}dt \equiv -\Phi(\rho^*)dz. \quad (1.2)$$

Integration of (1.2) yields  $\rho^*(z)$ , which should satisfy the conditions  $d\rho^*/dz < 0$  and  $\rho^*(z) \rightarrow \rho_{02}$  as  $z \rightarrow \infty$ .

The connection between the deviators is written by analogy with the Prandtl-Reiss elastic-plastic model, hence the condition for loading emergence on the surface has the form

$$T^{ik}T_{ik} = f^2(p, \rho), \quad (1.3)$$

where  $T^{ik}$  is the stress deviator and  $f(p, \rho) = \kappa(p, \rho)p$ . The function  $\kappa(p, \rho)$  is selected so as to transfer a diminution in the internal friction coefficient as the medium loosens and goes over to a liquid model at high pressures. The possibility of computing the motion of nonrocky soils by more simple models is embedded in the program. In a strong explosion the nearby zone is considered in a gasdynamic approximation by the equation of state of Mie-Gruneisen type with the thermal part of the pressure taken into account.

2. A difference methodology for solving the equations of motion of a continuous medium is created to analyze underground explosions with the proposed soil model. The initial differential equations are written in a mixed Euler-Lagrange system of coordinates, analogous to that proposed in [2]. This system is formed by closed Lagrange lines  $r = \text{const}$  and rays emerging from a common center  $\vartheta = \text{const}$ .

The selection of such a system is due first to the geometry of the problems being computed and, secondly, to the presence of contact boundaries. Moreover, the difference schemes using a purely Lagrangian representation of motion describe the behavior of free and contact boundaries poorly.

The spherical  $(R, \varphi, \psi)$  coordinate system with center in a cavity filled initially with explosion products is selected as the external (fixed) coordinate system.

With respect to the solution of the differential equations, it is assumed that it possesses axial symmetry. All this permits writing the relation between the external and the computational coordinate systems in the form

$$R = R(r, \vartheta, t), \quad \varphi = \vartheta.$$

The components

$$u = u^r \partial R / \partial r, \quad v = u^\vartheta$$

are selected as the desired velocities, where  $u^r$ ,  $u^\vartheta$  are the contrainvariant components of the velocity vector.

The selection of such variables assures the continuity of the velocity components of  $u$  on the contact boundary and reduces the question of the approximation of the transfer term to an equation for

$$\partial R / \partial t = v \partial R / \partial r.$$

Analogous considerations specify the selection of the stress tensor components  $p^{ik}$ , and the relation between the contravariant and the "computed" constituents is given by the relationships

$$p^{11} = (R_r)^2 p^{rr}, p^{12} = R_r p^{r\theta}, p^{22} = p^{\theta\theta}, p^{33} = p^{\psi\psi}$$

(here  $p^{rr}$ ,  $p^{r\theta}$ ,  $p^{\theta\theta}$ ,  $p^{\psi\psi}$  are contravariant constituents).

Hence  $p^{ik} = -p g^{ik} + T^{ik}$ , where  $p$  is the pressure,  $G = \{g^{ik}\}$  is the metric tensor, and  $T = \{T^{ik}\}$  is the stress deviator.

The stress state in the soil model considered depends on the loading history, i.e., there is the need to follow individual particles of the medium. Hence, a third coordinate system, a Lagrangian system, is introduced; the coordinate  $r$  was introduced earlier, and the transfer equation

$$\partial \chi / \partial t + v \partial \chi / \partial \theta = 0$$

is satisfied for the other coordinate  $\chi$ , corresponding to particle motion in the channel formed by the Lagrangian lines  $r = \text{const}$ .

Therefore, the method uses three coordinate systems: external, spherical ( $R, \varphi$ ), computed ( $r, \theta$ ), and Lagrangian ( $r, \chi$ ).

The complete system of equations becomes

$$\begin{aligned} \frac{\partial u}{\partial t} + 2v \frac{\partial u}{\partial \theta} - 2uv \frac{R_\theta}{R} + v^2 \frac{RR_{\theta\theta} - 2R_\theta^2 - R^2}{R} = -g \left( \cos \theta + \frac{R_\theta}{R} \sin \theta \right) + \frac{1}{\rho} \left[ \frac{\partial p^{11}}{\partial R} + \frac{1}{\sin \theta} \frac{\partial (p^{12} \sin \theta)}{\partial \theta} \right. \\ \left. + \frac{2}{R} p^{11} + 2 \frac{\partial R_\theta}{\partial R} p^{12} + p^{22} \frac{RR_{\theta\theta} - 2R_\theta^2 - R^2}{R} + (R_\theta \sin \theta \cos \theta - R \sin^2 \theta) p^{33} \right], \\ \frac{\partial v}{\partial t} + v \frac{\partial v}{\partial \theta} + 2uv \frac{1}{R} + \frac{2R_\theta}{R} v^2 = -g \frac{\sin \theta}{R} + \frac{1}{\rho} \left[ \frac{\partial p^{12}}{\partial R} \right. \\ \left. + \frac{\partial (p^{22} \sin \theta)}{\partial \theta} \frac{1}{\sin \theta} + \frac{4p^{12}}{R} + \left( \frac{4R_\theta}{R} + \frac{\partial R_\theta}{\partial R} \right) p^{22} - p^{33} \sin \theta \cos \theta \right], \\ \frac{\partial \rho}{\partial t} + v \frac{\partial \rho}{\partial \theta} + \rho \frac{\partial v}{\partial R} = \rho \frac{\partial u}{\partial R} + \frac{2\rho u}{R} + \frac{2\rho v R_\theta}{R} + \rho v \cot \theta = 0, \\ \frac{\partial T}{\partial t} = u, \quad \frac{\partial \chi}{\partial t} + v \frac{\partial \chi}{\partial \theta} = 0, \quad \frac{d\rho}{dt} = K \left[ \frac{1}{\rho} \frac{d\rho}{dt} + \Phi(\rho, \rho) \right] \bar{J}_2, \quad \dot{\lambda} T + \frac{dT}{dt} = -2\mu V_{\cdot\cdot} \left( \frac{dT}{dt} \right)_r \end{aligned} \quad (2.1)$$

where  $g$  is the free-fall acceleration;  $\rho$ , density;  $p$ , pressure;  $T$ , stress deviator;  $V$ , strain rate deviator;  $(dT/dt)_r$ , tensor corresponding to the change in stress state because of rotation of a material particle (the form of this tensor will be presented below). The coefficient  $\lambda$  differs from zero for inelastic stress and  $\mu$  is the shear modulus.

The boundary conditions for the system of equations presented are given on the boundary of the cavity, on the free surface, and on some line sufficiently far from the center of the explosion. All these boundaries coincide with the Lagrangian lines  $r = \text{const}$ .

The initial system of differential equations (2.1) is approximated by a system of explicit difference equations. The domain of the solution in the planes ( $r, \theta$ ) and ( $r, \chi$ ) is hence partitioned into rectangular cells.

The cells coincide at the initial instant, and one mesh later start to move relative to one another. The separation of the computed quantities is shown in Fig. 2, where ABCD is the computed cell,  $A_1, B_1, C_1, D_1$  is the Lagrangian cell, BC is an  $r$ -coordinate line, AB is a  $\theta$ -coordinate line, the point EC is the center of the computed cell, and EL is the center of the Lagrangian cell.

The transfer terms in the difference equations are approximated by one-sided differences taking account of the sign of the velocity  $v$ ; the remaining derivatives with respect to the space are approximated by central differences. The difference equations are not presented because of awkwardness. The order of determining the desired mesh functions is the following:

$$\begin{aligned} u^{n+1} &= f_1 \left( u^n, v^n, p^{11n}, \rho^n, R^n, \tau \right), \\ v^{n+1} &= f_2 \left( u^n, v^n, p^{12n}, \rho^n, R^n, \tau \right), \\ R^{n+1} &= f_3 \left( u^{n+1}, R^n, \tau \right), \quad \chi^{n+1} = f_4 \left( v^{n+1}, \chi^n, \tau \right), \end{aligned}$$

where  $\tau$  is the time spacing.

The components of the strain rate deviator  $\left\{V^{ik}\right\}^{n+1}$  at the middles of the computed cells are determined by means of the computed velocities. The components of the velocity deviator at the middles of the Lagrangian cells must be known to determine the stress tensor. These components can be obtained by a parallel transfer of the velocity deviator from the adjacent computed cells. To  $(\Delta\vartheta)^2$  accuracy, the parallel transfer reduces to a simple component-by-component interpolation of the strain rate deviator.

By knowing the new position of the Lagrangian cells (the coordinates  $\left(\frac{x}{\chi}\right)^{n+1}$ ), their volume and, therefore, their density, can be determined. In particular, the volume can be determined by means of the addition formula

$$\Delta W^{n+1} = -2\pi/3 (\Delta R^3) (\Delta \cos \vartheta), \quad \rho^{n+1} = M/\Delta W,$$

where M is the mass enclosed in the Lagrangian cell.

The new stress state in the middles of the Lagrangian cells is determined in conformity with the equations of state. If formula (1.1) is valid for the pressure in any coordinate system, then the tensor relationship

$$\lambda T + dT/dt = 2\mu V + (dT/dt)_R, \quad (2.2)$$

is valid for the stress deviator.

The coefficient  $\lambda$  is different from zero when the point in stress space falls on the loading surface (1.3). In this case, the deviator components  $\tilde{T}^{ik}$  obtained from (2.2) for  $\lambda = 0$  are multiplied by a certain constant C such that the image point remains on this surface, or in other words, the constant C is determined from the equation

$$C^2 \tilde{T}^{ik} \tilde{T}_{ik} = f(p, \rho), \quad \text{if } \tilde{T}^{ik} \tilde{T}_{ik} > f(p, \rho).$$

The component  $(dT/dt)_R$  is associated with the condition when, returning with an angular velocity  $\omega$ , the particle tensor of the direction also returns with the same angular velocity. It can be shown that this tensor is expressed through the tensor T and the coaxial tensor  $\Omega$  by the following:

$$(dT/dt)_R = T * \Omega - \Omega * T,$$

where the asterisk denotes the convolution relative to one pair of subscripts.

The components of the tensor  $\Omega$  in our coordinate system have the form

$$\Omega = \begin{pmatrix} 0 & -\omega/\sqrt{g_0} & 0 \\ \omega/\sqrt{g_0} & 0 & 0 \\ 0 & 0 & 0 \end{pmatrix}, \quad g_0 = \|G\|,$$

$$\omega = 0,5 \left( \frac{\partial(u - R_0 v)}{R \partial u} - \frac{R_0}{R} \frac{\partial(u - R_0 v)}{\partial R} - R \frac{\partial v}{\partial R} \right) - v.$$

The expression for the total derivative  $dT/dt$  includes the derivatives of the basis vectors with respect to the time also [3]. Let us present the complete expression for the determination of  $T^{11}$ , say

$$\frac{dT^{11}}{dt} = 2\mu T^{11} + T^{11} \frac{2R_0}{R} (v + \omega) + T^{12} 2R \left[ \omega \left( 1 + \frac{R_0^2}{R^2} \right) + v \left( 1 + \frac{2R_0^2}{R^2} \right) - \frac{1}{R} \frac{\partial(u - R_0 v)}{\partial \vartheta} + \frac{R_0}{R} \frac{\partial v}{\partial \vartheta} + \frac{R_0}{R^2} u \right].$$

The stress tensor is constructed by means of the newly computed pressure and stress deviator components, and is then interpolated to the middles of the computed cells.

To compute the shocks artificial viscosity in invariant form is added to the pressure:

$$q = q_1 c_L^2 \frac{d\rho}{dt} \tau + q_2 \rho \left[ \min \left( \Delta R \frac{\partial(u - R_0 v)}{\partial R}, 0 \right)^2 + \min \left( \Delta \vartheta \frac{dv}{\partial \vartheta}, 0 \right)^2 \right].$$

Moreover, terms of the form  $\partial^2 u / \partial R^2$ ,  $\partial^2 u / \partial \vartheta^2$ , etc. with coefficients proportional to the time spacing  $\tau$  are added to the right sides of the equations for u and v. These terms perform the same role as does the viscosity tensor in the method in [4].

3. The possibilities of the method and the equation of state described above for the soil can be illustrated by the results of computations of the following problems.

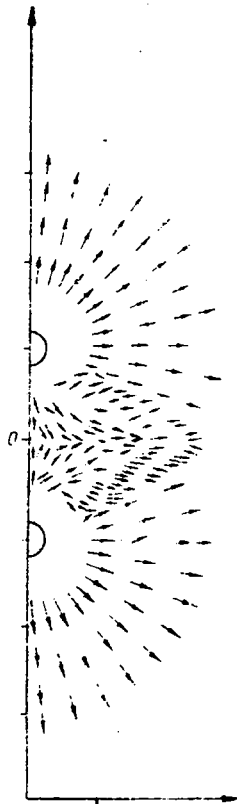


Fig. 3

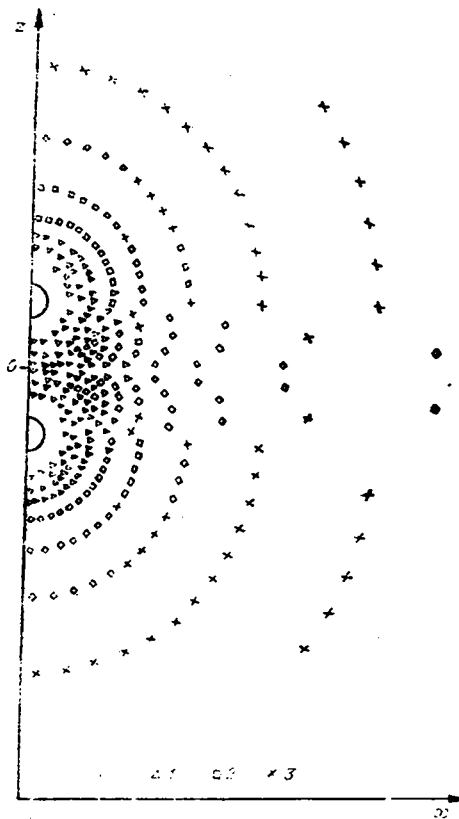


Fig. 4

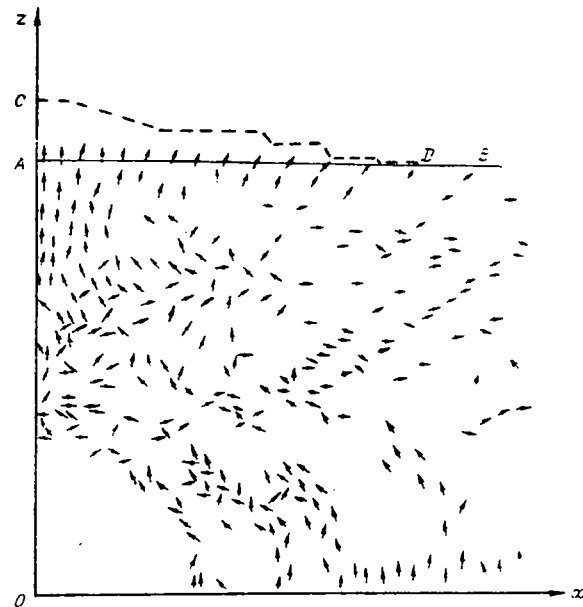


Fig. 5

Computation of the Simultaneous Explosion of Two Charges. The explosion of two charges separated by the distance  $l$  can be considered as the explosion of one charge, removed a distance  $l/2$  from the rigid wall. (The plane of symmetry, equally remote from both charges, is naturally considered as a rigid wall since there are no normal displacements thereon.) Unique effects caused by the interaction of the stress fields of the adjacent charges occur in a pairwise explosion. Among such effects might be the distortion of the spherical shape of the camouflet cavity, the change in configuration of the destruction zones in comparison with a spherically symmetric explosion, the closure of the cavities, and the extrusion of the soil from the region between

the charges. The parameters of the soil equation of state correspond to granite in the computation performed. The energy of the explosion in the initial state is distributed uniformly over the volume of a sphere with the reduced radius  $1.84 \text{ m/kT}^{1/3}$ , which corresponds to the radius of the evaporation zone in granite determined by Butkovich [5]. The explosion products are considered an ideal gas with  $\gamma=5/3$ . The results of the computations are presented in Figs. 3 and 4. The characteristic velocity field caused by the wave interaction is shown in Fig. 3. The destruction zones for the computation with a reduced separation of the charges  $52 \text{ m/kT}^{1/3}$  are displayed in Fig. 4 (1 is for soil destroyed by shear stresses, 2 is soil destroyed by tensile stresses, and 3 is undestroyed substance).

**Computation of a Loosening Explosion.** The formation of hillocks from destroyed and loosened rock [6] is observed in an explosion in dry rubble with a reduced depth of embedding above  $60 \text{ m/kT}^{1/3}$ . The singularity of a loosening explosion is the predominance of the fission mechanism in the formation of a true funnel. The gas acceleration phase is less definite, which permits termination of the computation at comparatively small displacements of the free surface. The computation of an explosion in granite with a reduced degree of embedding,  $84 \text{ m/kT}^{1/3}$ , was performed. The problem was computed up to the completion of cavity and destruction zone formation. The steady boundary of the fission funnel and the velocity field in the soil are shown in Fig. 5 (AB is the bottom surface, CD is the profile of the pile, but the camouflet cavity is not shown). The shape of the pile obtained as a result of the computation (Fig. 5) recalls the loosening hillock in the explosion "Salki," however, "levitation" of the cavity along the cave-in column, which results in funnel formation at the center of the pile in a natural explosion, was not taken into account in the computation.

#### LITERATURE CITED

1. V. N. Nikolaevskii, "On the relation between volume and shear plastic strains and on shocks in soft soils," *Dokl. Akad. Nauk SSSR*, 177, No. 3, (1967).
2. V. E. Neuvazhaev, V. D. Frolov, and N. N. Yanenko, "Equations of motion of a heat-conducting gas in mixed Euler-Lagrange coordinates," in: *Numerical Methods in the Mechanics of Continuous Media* [in Russian], Vol. 3, No. 1, Vychisl. Tsentr Sib. Otd, Akad. Nauk SSSR, Novosibirsk (1970).
3. L. I. Sedov, *Introduction to the Mechanics of a Continuous Medium* [in Russian], Fizmatgiz, Moscow (1962).
4. M. L. Wilkins, "Analysis of elastic-plastic flows," in: *Calculational Methods in Hydrodynamics* [Russian translation], Mir, Moscow (1967).
5. T. R. Butkovich, "Calculation of the shock wave from an underground nuclear explosion in granite," *J. Geophys. Res.* 70, 885-892 (1965).
6. V. N. Rodionov, V. V. Adushkin, V. N. Kostyuchenko, V. N. Nikolaevskii, A. N. Romashov, and V. M. Tsvetkov, *Mechanical Effect of an Underground Explosion* [in Russian], Nedra, Moscow (1971).